ognized. Analysis of human serums from 150 individuals in contact with cattle either as a result of working in slaughterhouses, or on dairy farms, has revealed no detectable antibody to BLV p24.

The incidence of bovine lymphosarcoma is currently estimated as around 20 per 100,000 for dairy cattle, and somewhat lower for beef cattle (*6*). Several countries have undertaken leukosis eradication campaigns or have attempted to eliminate the importation of cattle and semen from any but leukosis-free herds (*7*). This is primarily because of evidence that BLV can be spread horizontally (*6, 17*) and because epidemiologic studies indicate that in certain situations the incidence of bovine lymphosarcoma may be increasing (*18*). While the potential hazard of this virus to humans has not been fully evaluated, one recent report has indicated the development of leukemia in chimpanzees fed milk from clinically diseased cattle (*19*).

Serologic techniques, including immunodiffusion, complement fixation (*9*), and fluorescent antibody techniques (*8*) for the detection of BLV infection have offered important adjuncts to current clinical methods of disease detection which rely primarily upon hematological tests for persistent lymphocytosis. Comparison of existing immunologic methods with those described here are currently in progress. However, radioimmunoassays have in the past invariably proved to be more sensitive and specific for antibody detection than other immunologic procedures. The radioimmunoassay for BLV described herein should be useful in future epidemiologic studies in which the magnitude of BLV infection in cattle must be ascertained. Moreover, it should now be possible to estimate more thoroughly the potential hazard of this virus to humans through radioimmunologic analysis of serums from humans most likely to be at risk.

SUSHILKUMAR G. DEVARE
JOHN R. STEPHENSON
PADMAN S. SARMA
STUART A. AARONSON
Laboratory of RNA Tumor Viruses, National Cancer Institute, Bethesda, Maryland 20014
SATISH CHANDER
Animal Disease Research Institute, Ottawa, Ontario, Canada K2H 8P9

References and Notes

1. L. Gross, *Proc. Natl. Acad. Sci. U.S.A.* **71**, 2013 (1974); M. M. Lieber and G. J. Todaro, in *Cancer: A Comprehensive Treatise*, F. F. Becker, Ed. (Plenum Press, New York and London, 1975), vol. 2; S. A. Aaronson and J. R. Stephenson, *Biochim. Biophys. Acta. Rev. Cancer*, in press.
2. J. M. Miller, L. D. Miller, C. Olson, K. G. Gillette, *J. Natl. Cancer Inst.* **43**, 1297 (1969); S. K. Dutta, V. L. Larson, D. K. Sorensen, V. Perman, A. F. Weber, R. F. Hammer, R. E. Shope, Jr., in *Comparative Leukemia Research*, R. M. Dutcher, Ed. (Karger, New York, 1970), p. 548; T. G. Kawakami, A. L. Moore, G. H. Theilen, R. J. Munn, in *ibid.*, p. 471.
3. R. M. Dutcher, E. P. Larkin, R. R. Marshak, *J. Natl. Cancer Inst.* **33**, 1055 (1964).
4. L. D. Miller, J. M. Miller, C. Olson, *ibid.* **48**, 423 (1972).
5. C. Olson, L. D. Miller, J. M. Miller, H. E. Hoss, *ibid.* **49**, 1463 (1972); M. J. Van Der Maaten and J. M. Miller, *Bibl. Haematol. (Pavia)* **43**, 377 (1976).
6. J. E. Croshaw, Jr., D. A. Abt, R. R. Marshak, W. C. D. Hare, J. Switzer, J. Ispen, R. M. Dutcher, *Ann. N.Y. Acad. Sci.* **108**, 1193 (1963); G. H. Theilen, R. D. Appleman, H. G. Wixom, *ibid.*, p. 1203; G. Migaki, *Natl. Cancer Inst. Monogr.* **32**, 121 (1969).
7. H. J. Bendixen, *Off. Int. Epizoot. Bull.* **62**, 675 (1964).
8. J. F. Ferrer, L. Avila, N. D. Stock, *Cancer Res.* **32**, 1864 (1972).
9. J. M. Miller and C. Olson, *J. Natl. Cancer Inst.* **49**, 1459 (1972); J. M. Miller and M. J. Van Der Maaten, *ibid.* **53**, 1699 (1974).
10. H. J. Bendixen, *Ann. N.Y. Acad. Sci.* **108**, 1241 (1963).
11. H. Tabel, S. Chander, M. J. Van Der Maaten, J. M. Miller, *Can. J. Comp. Med.* **40**, 350 (1976).
12. M. J. Van Der Maaten, J. M. Miller, A. D. Boothe, *J. Natl. Cancer Inst.* **52**, 491 (1974).
13. U. K. Laemmli, *Nature (London)* **227**, 680 (1970).
14. F. C. Greenwood, W. M. Hunter, J. S. Glover, *Biochem. J.* **89**, 114 (1963).
15. H. C. McDonald, D. C. Graves, J. F. Ferrer, *Cancer Res.* **36**, 1251 (1976); R. V. Gilden, C. W. Long, M. Hanson, R. Toni, H. P. Charman, S. Oroszlan, J. M. Miller, M. J. Van Der Maaten, *J. Gen. Virol.* **29**, 305 (1975).
16. J. R. Stephenson and S. A. Aaronson, *J. Virol.* **12**, 564 (1973).
17. C. E. Piper, D. A. Abt, J. F. Ferrer, R. R. Marshak, *Cancer Res.* **35**, 2714 (1975).
18. S. M. Stamatovic and M. J. Jovanovic, *Bibl. Haematol. (Pavia)* **31**, 194 (1968).
19. H. M. McClure, M. E. Keeling, R. P. Custer, R. R. Marshak, D. A. Abt, J. F. Ferrer, *Cancer Res.* **34**, 2745 (1974).
20. Obtained from R. Wilsnack through the Office of Resources and Logistics, National Cancer Institute.
21. Obtained from ADRI, Ottawa, Canada.
22. Supported in part by contracts N01-CP-61024 and N01-CP-4-3254 of the Virus Cancer Program of the National Cancer Institute. We thank G. Caldwell, Communicable Disease Center, Atlanta, Georgia, for supplying human serums. S. Devare is a visiting fellow of the National Institutes of Health. We thank M. Van Der Maaten and J. Miller of USDA, Ames, Iowa, for providing the BLV-infected fetal lamb spleen cultures.

30 August 1976

Field Focusing Nuclear Magnetic Resonance (FONAR): Visualization of a Tumor in a Live Animal

Abstract. *A nuclear magnetic resonance (NMR) image of a tumor in a live animal is reported. The field focusing NMR method or* FONAR *process that now achieves the tumor outline is described.*

Since the introduction of the nuclear resonance technique for detecting cancer by Damadian (*1*), many other investigators (*2, 3*) have extended the observation, including Weisman *et al.* who demonstrated its utility in vivo by detecting a tumor on the tail of a live mouse (*3*). The method of Damadian, originally conceived for the detection of internal neoplasms in humans, achieved its objective by focusing the nuclear magnetic resonance (NMR) signal within the interior of the live host. The focused NMR signal was thereby externally directed to any internal location in the live subject for data acquisition. The focusing NMR technique (called FONAR) was developed in 1972 (*4*).

FONAR should be distinguished from various nonfocusing methods that have appeared since. A promising modification of the projection analysis methods is the Fourier transform imaging technique by Kumar, Welti, and Ernst (*5*). Focusing NMR permits the operator to externally direct the NMR spot to the anatomic site of interest for firsthand inspection of the signal characteristics at a suspicious locus. Furthermore, field focusing allows the NMR signal behavior of each anatomic region to be continuously monitored during the data acquisition phase of the FONAR imaging process.

In principle, focusing NMR is achieved by field regulation of the spatial boundaries of a signal-producing region inside a sample. This is accomplished by shaping the magnetic fields (H_0 and H_1) across the entire sample so as to construct a small resonant window within the sample, such that the ratio of the spin moment of the nucleus to its gyric moment is everywhere satisfied by the static and time varying H fields and is everywhere dissatisfied beyond its boundaries. In practice, both the static H_0 field and the inductive component of the radio frequency (rf) field (H_1) are shaped. The

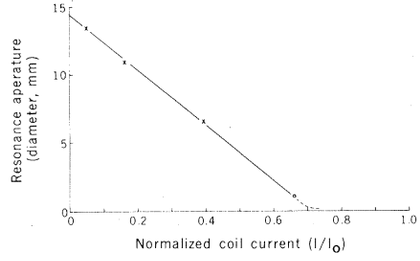

Fig. 1. Resonance aperture versus coil current. The o point shown is the extrapolated normalized current value for a 1-mm aperture.

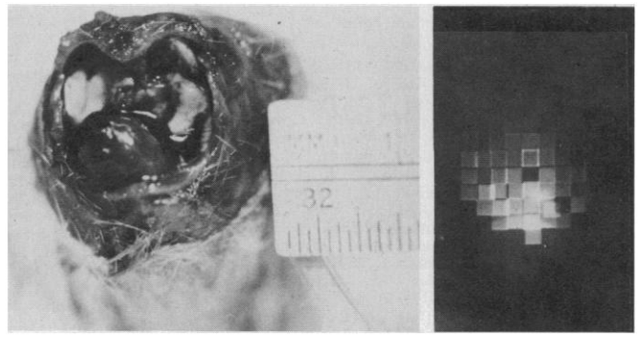

Fig. 2. Cross-sectional video FONAR image of a live mouse, obtained with a 3-mm exploring spot. At the left is a photograph of the anatomical section for comparison. The heart is anterior in the photo, and the lungs, seen as collapsed white structures, fill the remainder of the thorax. The most intense proton signal in the FONAR image occurs in the region of the blood-filled heart. The dark fields in the upper half of the photo were generated by the hydrogen-poor air-filled lungs. The television raster is seen coursing through the image. Overlap artifacts appear in the image as bright, vertical and horizontal lines and are due to imperfect positioning of adjacent mapping squares.

system of field correction coils for shaping H_0 was determined from the series solution of the Laplace equation in spherical coordinates,

$$\psi(r, \theta, \phi) = \sum_{m,n} \left(\frac{r}{a}\right)^n P_n^m(\cos\theta) [A_{mn}\cos m\phi + B_{mn}\sin m\phi]$$

where ψ is the scalar potential; r, θ, and ϕ are the spherical coordinates, with P_n^m the associated Legendre polynomials (*6*). The axial magnetic induction B_z of the coil system is then computed from the scalar potential using $B = -\nabla\psi$ for the case where the curl of B is taken as zero outside the surface enclosed by the coils. The field B_z can then be expanded in the derivatives of ψ. A linear combination of terms of the B_z expansion provides the H_0 field-regulating system that, together with H_1 shaping, controls the resonating volume, or resonance aperture in three dimensions (*7*).

We estimated the size of the resonance aperture achieved by our focusing technique as follows. A sample tube 19 mm (control) in inside diameter and filled with $NiCl_2$-doped water was placed in the NMR probe. The height of the free induction decay (FID) of the hydrogen signal after a 90° pulse was determined for a series of currents in the focusing coils and recorded. Phase adjustment was required for a maximum FID at each new current setting. The experiment was then repeated for a 13.5-mm (inside diameter) sample tube (experimental) and a plot was made of the ratio of signal intensities (FID amplitudes) generated by the control and experimental samples at each current setting. The current at which this intensity ratio attained a value of unity was taken as the current at which the diameter of the signal-producing region within the large tube equaled the inside diameter of the smaller tube. The coil current at the unity point, therefore, specified the current needed to produce a resonance aperture of diameter equal to the inside diameter of the experimental tube. At lesser currents, the resonance aperture exceeded the diameter of the smaller tube, the larger tube therefore generated more signal than the smaller, and the intensity ratio exceeded 1. The coil current required to achieve a unity intensity ratio for an 11- and 6.5-mm tube was also determined. A plot of tube diameters as a function of the normalized coil current (Fig. 1) generated an extrapolated estimate of the current required to achieve the 1-mm resonance aperture used in animal imaging.

The scan for developing the FONAR image moves the resonance aperture through an anatomic cross section, either by moving the animal with respect to the aperture or by moving the aperture, with the animal being held stationary. The method provides visible proton signal, without signal processing, from scanning apertures that are approximately spherical and estimated at slightly less than 1 mm.

The televised output is a stored video record of proton signal intensities (FID amplitudes) at various xy coordinates, generated by the resonance aperture as it was swept through a cross section of the animal's torso. While it was not so applied in this instance, the technique is readily adaptable to constructing images from T_1 (spin lattice relaxation) or T_2 (spin-spin relaxation) data taken at each of the FONAR loci of the scan. The Freeman-Hill method of progressive saturation (*8*) for obtaining T_1 is well suited to this purpose.

Video FONAR images were obtained in a CSCC (Canada Superconductor) superconducting magnet with the use of a SEIMCO (New Kensington, Pennsylvania) model RD variable frequency pulse spectrometer operating at 10 Mhz. The animal was successfully immobilized in the probe for 4 hours with 0.2 ml of valium (5 mg/ml) injected intraperitoneally. Figure 2 is a direct televised image of a section through the thorax of a live mouse at the level of the mediastinum. A photo of the postmortem anatomic section at the level of the cross-sectional image is in the left of the figure for direct comparison. The heart is anterior in the photo and the lungs, seen as collapsed white structures, fill the remainder of the thorax. A 3-mm scanning aperture was used. The most intense proton signal occurs in the region of the blood-filled heart. The signal-deficient dark fields in the upper half of the photo were generated by the proton-poor air-filled lungs. The television raster is seen coursing through the image. Overlap artifacts, appearing in the image as bright vertical and horizontal lines, are due to imperfect positioning of adjacent mapping squares.

Shown on the cover of this issue is a color video FONAR image of a cross section through the upper thorax (above the mediastinum) of a mouse that had a solid Ehrlich ascites tumor surgically implanted in the anterior chest wall. Each colored area designates a different range of signal amplitude. The anterior orange-pink and red region (at the bottom of the image), not present in normal control mice and indicative of a signal-producing mass, corresponds with the location of the tumor. The resolving limitation of a 1-mm scanning aperture in a 13-mm sample (thorax diameter) overestimates the tumor size partially obscuring the underlying lung fields. In the normal animal (not shown), the anterior half of the thorax appears as a blue signal-poor region representing the lung cavities. Having originally introduced the NMR method chiefly for the purpose of noninvasively detecting internal tumors in humans, we have succeeded in obtaining the first images of a tumor in a live animal.

RAYMOND DAMADIAN
LAWRENCE MINKOFF
MICHAEL GOLDSMITH
MICHAEL STANFORD
JASON KOUTCHER

Biophysical Laboratory, State University of New York at Brooklyn, 450 Clarkson Avenue, Brooklyn, New York 11203

References and Notes

1. R. Damadian, *Science* **171**, 1151 (1971).
2. H. E. Frey, R. R. Knispel, J. Kruuv, A. R. Sharp, R. T. Thompson, M. M. Pintar, *J. Natl. Cancer Inst.* **49**, 903 (1972); G. P. Raaphorst, J. Kruuv, H. Frey, in *The Nuclear Resonance Effect in Cancer*, R. Damadian, Ed. (Pacific Press, New York, in press); C. F. Hazlewood, D. C. Chang, D. Medina, G. Cleveland, B. L. Nichols, *Proc. Natl. Acad. Sci. U.S.A.* **69**, 1478 (1972); G. L. Cottam, A. Vasek, D. Lusted, *Res. Commun. Chem. Pathol. Pharmacol.* **4**, 495 (1972); R. G. Parrish, R. J. Kurland, W. W. Janese, L. Bakey, *ibid.* **183**, 438 (1973); D. P. Hollis, L. A. Saryan, H. P. Morris, *Johns Hopkins Med. J.* **131**, 441 (1972); D. P. Hollis, J. S. Economou, L. C. Parks, J. C. Eggleston, L. A. Saryan, J. L. Czeisler, *Cancer Res.* **33**, 2156 (1973); R. A. Floyd, J. S. Leigh, B. Chance, M. Miko, *ibid.* **34**, 89 (1974); I. C. Kiricuta, D. Demco, V. Simplaceanu, *Arch. Geschwulstforsch.* **42**, 226 (1973); R. E. Block, *FEBS Lett.* **34**, 109 (1973); W. R. Inch, J. A. McCredie, R. R. Knispel, R. T. Thompson, M. M. Pintar, *J. Natl. Cancer Inst.* **52**, 353 (1974); W. Bovee, P. Huisman, J. Smidt, *ibid.*, p. 595; L. A. Saryan, D. P. Hollis, J. S. Economou, J. C. Eggleston, *ibid.*, p. 599; C. F. Hazlewood, G. Cleveland, D. Medina, *ibid.*, p. 1849; R. E. Block and G. P. Maxwell, *J. Magn. Reson.* **14**, 329 (1974); B. M. Fung, *Biochim. Biophys. Acta* **362**, 209 (1974); S. Ratkovic and C. Rusov, *Period. Biol.* **76**, 19 (1974); S. S. Ranade, S. S. Shah, K. S. Korgaonkar, C. V. Talwalkar, S. R. Kasturi, paper presented at the Fifth International Symposium on Magnetic Resonance, Bombay, India, 14 to 18 January 1974; C. F. Hazlewood, in *The Nuclear Resonance Effect in Cancer*, R. Damadian, Ed. (Pacific Press, New York, in press); I. D. Weisman, L. H. Bennett, L. R. Maxwell, in *ibid.*; W. Bovee and J. Smidt, in *ibid.*; N. Iijima, S. Saitoo, Y. Yoshida, N. Fujii, T. Koike, K. Osanai, K. Hirose, in *ibid.*; M. M. Pintar, in *ibid.*; S. Ratkovic and C. Rusov, in *ibid.*; S. S. Ranade, in *ibid.*; R. E. Gordon, J. R. Singer, L. Crooks, in *ibid.*; Z. Abe and K. Tanaka, in *ibid.*
3. I. D. Weisman, L. H. Bennett, L. R. Maxwell, M. W. Woods, D. Burk, *Science* **178**, 1288 (1972).
4. R. Damadian, U.S. Patent 3,789,832, filed 17 March 1972.
5. A. Kumar, D. Welti, R. R. Ernst, *Naturwissenschaften* **62**, 34 (1975).
6. P. M. Morse and H. Feshbach, in *Methods of Theoretical Physics II*, (McGraw-Hill, New York, 1953), p. 1265.
7. R. Damadian, in *The Nuclear Resonance Effect in Cancer*, R. Damadian, Ed. (Pacific Press, New York, in press).
8. R. Freeman and H. D. Hill, *J. Chem. Phys.* **54**, 3367 (1971).
9. Supported in part by grant R01-CA 14988-06 from the National Institute of Health.

23 July 1976; revised 24 September 1976

Hormonal Release of Programmed Behavior in Silk Moths: Probable Mediation by Cyclic AMP

Abstract. *The eclosion hormone triggers a stereotyped preprogrammed pattern of behavior in silk moths. The effects of the hormone were duplicated by the injection of dibutyryl adenosine 3',5'-monophosphate, adenosine 3',5'-monophosphate (cyclic AMP), or guanosine 3',5'-monophosphate (cyclic GMP) into theophylline-treated pharate moths. Treatment with theophylline reduced the latency of the response to a low dose of hormone, presumably by blocking phosphodiesterase. Endogenous levels of cyclic AMP, but not cyclic GMP, increased significantly in the central nervous system within 10 minutes after hormone injection. We conclude that an early step leading to the release of the eclosion motor program is an increase in cyclic AMP in target neurons of the central nervous system.*

In many animals, hormones can act rapidly to alter behavior (*1*). The exact mechanisms by which these behavioral changes come about are unknown, but it is likely that the initial responses in the nervous system are similar to those shown by nonneural tissues. In the case of peptide and amine hormones, these agents typically act at the surface of their target cells to alter the level of adenosine 3',5'-monophosphate (cyclic AMP) (*2*). Recently, guanosine 3',5'-monophosphate (cyclic GMP), has also been implicated in the action of certain hormones (*3*). We report here that cyclic nucleotides play a central role in the hormonal mediation of complex behavioral changes in a silk moth.

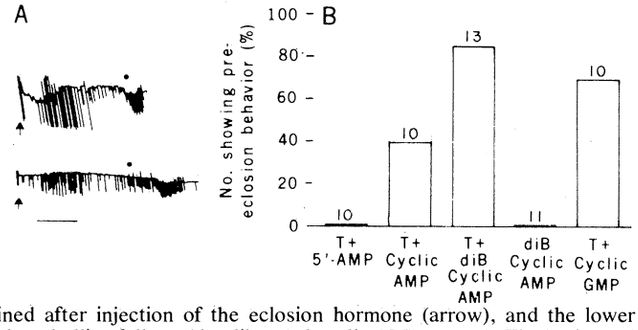

Fig. 1. The ability of cyclic nucleotides to stimulate preeclosion behavior when injected into isolated abdomens of pharate *H. cecropia* moths. (A) Tracings of movement were recorded by attaching the tip of the abdomen to a lever that wrote on a revolving drum (5); the upper tracing was obtained after injection of the eclosion hormone (arrow), and the lower tracing after injection of theophylline followed by dibutyryl cyclic AMP (arrow). The horizontal line equals 0.5 hour; the dot identifies the onset of the peristaltic movements. (B) The percentage of abdomens showing the preeclosion behavior after injection of 1 mg of a nucleotide. Theophylline (50 μg) was injected at *T*, 5 minutes before nucleotide injection; *AMP*, adenosine monophosphate; *diB-cyclic AMP*, dibutyryl cyclic AMP. The number gives the size of each group.

In the pharate (*4*) stage of the moth *Hyalophora cecropia*, a brain-derived hormone, the eclosion hormone, triggers a species-specific sequence of motor acts that culminates in the moth's escape from the pupal cuticle (eclosion) and the activation of its repertoire of adult behavior (*5*). The first portion of the emergence sequence, the preeclosion behavior (Fig. 1A) begins about 10 to 15 minutes after hormone application. It consists of three phases: an initial 0.5-hour period of frequent abdominal rotations; a period of quiescence of about the same duration; and, finally, a second hyperactive period during which strong peristaltic contractions move anteriorly along the abdomen to cause eclosion. Experiments on deafferented abdominal nervous systems and on isolated abdominal nervous systems indicate that the information for the pattern of preeclosion behavior is preprogrammed in the abdominal ganglia and that this behavioral program is triggered by the direct action of the hormone on the abdominal central nervous system (CNS) (*6*).

Since the eclosion hormone appears to be proteinaceous (*7*), we sought to determine whether its effects are exerted by way of changes in cyclic nucelotide levels. To guard against our treatments causing a release of endogenous hormone from the brain, abdomens isolated from pharate adults were routinely utilized (*8*). The behavior of each abdomen was continuously monitored by attaching the tip of the abdomen to a lever that wrote on a revolving drum; preparations were also inspected at 10- to 15-minute intervals. The preeclosion behavior was recognized by the characteristic temporal pattern of activity coupled with the appearance of the distinctive peristaltic movements during the final phase.

The effects of injecting one of four purine nucleotides (*9*) into isolated abdomens of *H. cecropia* are summarized in Fig. 1. Before the nucleotides were injected, theophylline [Sigma; 50 μg in 10 μl of Ringer (*10*) solution] was injected to inhibit the high cyclic nucleotide phosphodiesterase activity in moth nervous tissue (*11*). Dibutyryl cyclic AMP [which may enter cells more readily, or have greater resistance to phosphodiesterase than cyclic AMP (*2*)] released the preeclosion behavior in 11 of 13 abdomens. Cyclic AMP was somewhat less active whereas 5'-adenosine monophosphate was inert. Injections of cyclic